Attractor reconstruction from interspike intervals is incomplete

Tomáš Gedeon Matt Holzer [1] Mark Pernarowski

Department of Mathematical Sciences, Montana State University, Bozeman, MT 59715

Abstract

We investigate the problem of attractor reconstruction from interspike times produced by an integrate-and-fire model of neuronal activity. Suzuki *et. al.* [14] found that the reconstruction of the Rössler attractor is incomplete if the integrate-and-fire model is used. We explain this failure using two observations. One is that the attractor reconstruction only reconstructs an attractor of a discrete system, which may be a strict subset of the original attractor. The second observation is that for a set of parameters with nonempty interior numerical simulations demonstrate that the attractor of the discrete system is indeed a strict subset of the Rössler attractor. This is explained by the existence of phase locking in a nearby periodically forced leaky integrate-and-fire model.

Key words: Attractor reconstruction; integrate-and-fire neuron; Rössler attractor; phase locking

1 Introduction

The idea of attractor reconstruction from time series data dates back to Packard *et. al.* [11] and was later put on firm mathematical footing by Takens [18] and Sauer *et. al.* [16]. Central to this technique is the assumption that the observed time series is generated by an attractor of a dynamical system on a finite dimensional manifold, and the goal is to understand properties of this attractor from the limited information provided by the time series. Such properties include the dimension of

the underlying attractor [19,8], characteristic exponents [4] and entropy [7]. Since time series data is ubiquitous in science, this area of research has drawn much attention in the past decade.

Among the outstanding problems in neuroscience is the question of neural coding: how is crucial information represented in the neural spike train? This question can be formulated as a problem of *neural decoding* which takes center stage in a recent book by Rieke *et. al.* [12]. Can we reconstruct sensory input by looking only at the spike trains emmited by the sensory neurons? Ideally, one would like to study the neural decoding problem for a rich stimulus such as that encountered in a neuron in its natural setting. Such a stimulus is usually characterized by its statistical properties and the investigation is focused on how these characteristics are related to statistics of the spike train(s) (see [1,5,17] and many others). In this paper we choose to take "rich stimulus" to mean a non-periodic stimulus generated by a chaotic attractor. This provides the link between time series reconstruction theory and the problem of neural decoding. The stimulus we consider does not have the observed statistics of the natural stimulus, but it has infinitely many Fourier components and this may justify calling it a rich stimulus. We arrive at the central question this paper wants to address: Can an attractor be fully reconstructed solely from the information encoded in the interspike intervals? The short answer to this question, in general, is no.

Using a signal garnered from the Rössler attractor, Suzuki *et. al.* [14] attempted to reconstruct dynamics on the Rössler attractor using a spike train collected from a neuron in the terminal ganglion of the cricket. That reconstruction was not complete. They also obtained similar results for the Rössler attractor when a leaky integrate-and-fire (IF) model was used in the reconstruction. The explanation by Suzuki *et. al.* [14] centered on an observation that an attractor of a certain discrete dynamical system seems to be a strict subset of the original Rössler attractor. The discrete system is defined in the following way. Take p_0 on the Rössler attractor and let $p(t)$ be a solution with initial condition $p(0) = p_0$. Let $g(p_0)$ be that point on $p(t)$ at the time t where the IF model first produces a spike. A trajectory $\{g^n(p_0)\}$ for a particular choice of p_0 is marked in Figure 1 for two different parameter sets. As we can see, the trajectory forms a strict subset of the Rössler attractor in both cases.

We have two goals in this paper. The first goal of the paper is to relate the attractor of the discrete map g to the problem of reconstruction of the entire attractor. Our main result here is that the *dynamical reconstruction*, which we describe in detail in section 5, can faithfully reconstruct only the attractor of the discrete system (i.e. in Figure 1 only the set of marked points). The second goal of this paper is to show that for an open set of parameters the attractor of the discrete system for interspike reconstruction is a strict subset of the Rössler attractor.

We also compare two different methods of dynamical recontruction. One is inter-

spike interval reconstruction and the other is *delay coordinate reconstruction*(Takens [18]). We show that the previous results of Takens [18] about delay coordinate reconstruction , when recast in our framework, imply that for delay reconstruction the attractor of the discrete systems coincides (generically) with the full attractor. This shows that the delay reconstruction will (generically) reconstruct the whole attractor.

We will now outline our argument in support of the second goal. The results of Keener *et. al.* [10] (see also results of Coombes and Bressloff [2,3]) show that phase locking occurs in the periodically forced IF model. This means that there are open regions in parameter space for which the number of fires per period of the forcing function is constant. These sets have a cusp shape and are sometimes called Arnold tongues [9]. Keener *et. al.* [10] has shown that the phase locking is related to constancy of a rotation number for a certain circle map.

We then observe that the Rössler attractor generated stimulus posseses a dominant Fourier mode. Then, we conjecture that in a neighborhood of an Arnold tongue of the IF model (periodically forced by the dominant Fourier mode) there should be a smaller open set of parameters where the corresponding Rössler driven IF model exhibits approximate phase locking. This would explain the behavior in Figure 1. To prove that our intuition is correct would require that we identify a large enough function space to contain both the Rössler produced input and its dominant Fourier component. Then we would have to generalize the continuity result for rotation numbers ([9]) from a space of continuous periodic functions with fixed period to this more general function space. Note that this also requires generalization of the concept of a rotation number (or firing rate) to non-periodic inputs. These concepts are currently under investigation, but beyond the scope of this paper.

We choose instead to show numerically that there is an open set of parameters where the Rössler driven IF model exhibits approximate phase locking. For each parameter value in this set the attractor of the discrete system is a strict subset of the Rössler attractor. This indicates that the dynamic interspike interval reconstruction does not work for an open set of parameters.

To find this set we first compute an analytical approximation of the $2 : 1$ Arnold tongue for the periodic case. We then numerically find the values in the neighborhood of this tongue for which the corresponding Rössler attractor stimulus generates a discrete attractor that is a strict subset of the total Rössler attractor.

The paper is organized as follows. In section 2, we review the definition of the Rössler attractor, define the integrate-and-fire (IF) model and review the results of Suzuki *et. al.* [14]. In section 3 we review results of Keener *et. al.* [10] on phase locking for the periodically forced IF model and compute an analytical approximation of the $2 : 1$ locking region. In section 4 we then present numerical evidence that there is an open set of parameters in the neighborhood of this tongue where the IF model when driven by the Rössler attractor exhibits approximate phase locking.

In section 5, theory is developed to link the attractor of the discrete system with the reconstruction. The manuscript is summarized by a conclusion which includes a discussion of some open questions.

2 Preliminaries

2.1 Periodically forced integrate and fire model

In the integrate-and-fire (IF) model ([6]), the state of a neuron is described by a variable $u(t)$ which can be thought of as either i) the membrane potential or ii) the percentage of sub-threshold voltage required to cause the neuron to elicit an action potential. In either interpretation the stimulus $s(t)$ at time t is integrated until $u(t)$ reaches some threshold Θ. When $u(t)$ reaches the threshold, then t is considered a firing time and $u(t)$ is reset instantaneously to zero. To make the model more realistic, leak dynamics are often included to simulate membrane permeabilities which cause the cell to repolarize. Mathematically, the model is described by the following equations:

$$\frac{du}{dt} = -\sigma u + s(t),$$
$$u(t) = \Theta \Rightarrow u(t^+) = 0 \tag{1}$$

In this paper we choose $\Theta = 1$.

For the periodically forced IF model $s(t) = S_P(t)$ where $S_P(t)$ is defined by

$$S_P(t) = S(1 + B\cos(t)) \tag{2}$$

and S and B are constants. Depending on the value of the parameters $\lambda = (\sigma, S, B)$, the model (1) can exhibit a variety of different dynamics, including phase locking where the solution $u(t)$ entrains to a periodic orbit whose period is commensurate to the forcing period. The dependence of this phase locking on λ will be explored in section 3.

2.2 Rössler Attractor forcing in the IF model

In this subsection we introduce the Rössler system and define how it is used to force the IF model. The Rössler system is defined by the following set of differential equations:

$$\frac{dx}{dt} = -(x + y)$$
$$\frac{dy}{dt} = x + ay$$
$$\frac{dz}{dt} = bx - cz + xz. \tag{3}$$

The Rössler attractor $\mathcal{A}$ for $(a, b, c) = (0.36, 0.4, 4.5)$ is illustrated in Figure 1. For the remainder of the paper we fix these values of (a, b, c).

The first component of the Rössler attractor $x(t)$ is scaled using constants $\hat{B}$ and $\hat{S}$ to produce an input signal $S_R(t)$:

$$S_R(t) = \hat{S}(1 + \hat{B}x(t)). \tag{4}$$

The integrate-and-fire model (1) with input $s(t) = S_R(t)$ produces a spike train, or, equivalently, a sequence of firing times $\{\tau_n\}_{n=1}^{\infty}$. Corresponding to each firing time, there is an associated point on $\mathcal{A}$. The sequence of such points is best described via a map g defined as follows:

Definition 1 ([14]) Let X be a compact neighborhood of the Rössler attractor $\mathcal{A}$. For each $p \in X$, set $u = 0$ and let $g(p) \in X$ be the point when the next spike is generated. More precisely, let $(p(t), u(t))$ be a solution of (1),(3) where $s(t) = S_R(t)$ from (4). Then $g(p) := p(\tau_1)$ where τ_1 is the smallest time such that $u(\tau_1) = 1$.

We note that the map g depends on the parameters $(\sigma, \hat{S}, \hat{B})$. For some choices of these parameters and some choices of initial conditions p we may have $u(t) < 1$ for all t. Therefore the domain of definition of g depends on parameters $(\sigma, \hat{S}, \hat{B})$, and it could be empty for some choice of parameters. The map g defines a discrete dynamical system on X. Obviously, since $\mathcal{A}$ is an invariant set of a continuous dynamical system, it is also an invariant set of the discrete system (X, g).

Shown in Figure 1, the orbits $\{g^n(p)\}_{n=0}^{\infty}$ are superimposed (points) on $\mathcal{A}$ for different $(\sigma, \hat{S}, \hat{B})$ values. For these parameter values, the numerical simulations suggest that the limit set $L_g(p)$ of the sequence $\{g^n(p)\}_{n=0}^{\infty}$ is a strict subset of the attractor $\mathcal{A}$. Moreover, repeated numerical simulations (not shown) for different initial conditions p reproduced five and two leaf patterns nearly identical to those observed in Figure 1a and Figure 1b, respectively. Suzuki et. al. [14] made the observation that the reconstruction of the Rössler attractor for these parameter values from spike train was poor.

The five and two leaf patterns shown in Figure 1 suggest a relationship to phase locking that might be observed when the IF model is periodically forced by the dominant Fourier mode of the forcing $S_R(t)$. This relationship is explored numerically in section 4. To make such comparisons, we first examine the case $s(t) = S_P(t)$ in section 3.
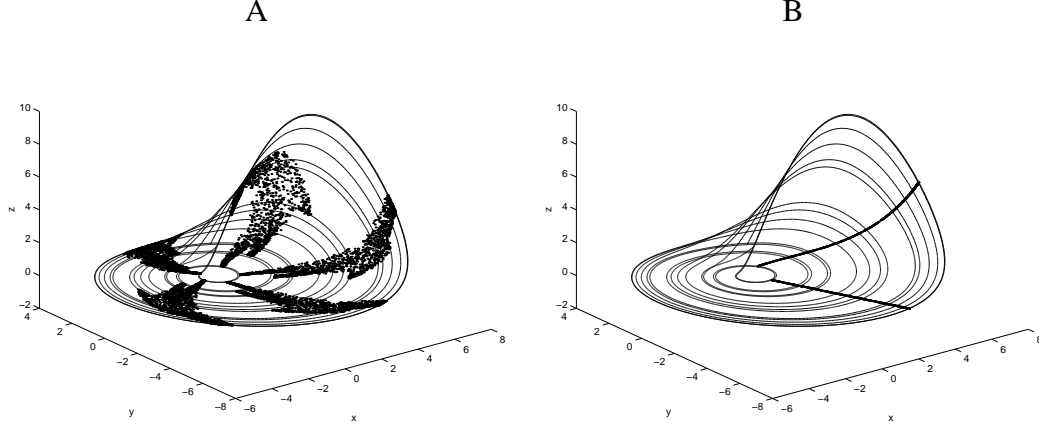
Fig. 1. Figure shows the firing locations generated by the integrate and fire model (points) superimposed on the Rössler attractor for A) $(\sigma, \hat{S}, \hat{B}) = (1.77, 2, 1/40)$ and B) $(\sigma, \hat{S}, \hat{B}) = (2, 2, 1/40)$.

3   Phase locking in the IF model

In this section we summarize some facts about phase locking in the periodically forced IF model and make some analytic extensions to previous work.

When $s(t) = S_P(t)$, Keener *et. al.* [10] showed (by integrating (1) over the range $u \in (0, 1)$) that consecutive firing times τ_n, $n = 0, 1, 2, \ldots$ are related via

$$F(\tau_{n+1}) = F(\tau_n) + \frac{\sigma}{S} e^{\sigma \tau_n}$$

where

$$F(\tau) \equiv e^{\sigma \tau} \left(1 - \frac{\sigma}{S} + B \sin \beta \sin(\tau + \beta)\right) \quad , \quad \sin \beta = \frac{\sigma}{\sqrt{1 + \sigma^2}}. \tag{5}$$

When $F(\tau)$ is invertible and defined on the range of $F(\tau) + (\sigma/S)e^{\sigma \tau}$, consecutive firing times are related by

$$\tau_{n+1} = f(\tau_n), \tag{6}$$

where the continuous function $f : \mathbf{R} \mapsto \mathbf{R}$ is defined by:

$$f(\tau) = F^{-1}\left(F(\tau) + \frac{\sigma}{S} e^{\sigma \tau}\right). \tag{7}$$

The function f satsifies $f(x + 2\pi) = f(x) + 2\pi$ and therefore is a *lift* of a circle map $h : \mathbf{S^1} \mapsto \mathbf{S^1}$ and the following diagram commutes

$$
\begin{array}{ccc}
\mathbf{R} & \xrightarrow{f} & \mathbf{R} \\
p \downarrow & & p \downarrow , \\
S^1 & \xrightarrow{h} & S^1
\end{array}
$$

where $p : \mathbf{R} \to S^1$ is a standard projection. One can then define a *rotation number*, ρ, as:

$$\rho(f) = \lim_{n \to \infty} \frac{f^n(\tau)}{2\pi n} \tag{8}$$

where $f^n(\tau) = \tau_n$ is the time of the n-th fire.

Definition 2 The periodically driven system (1) is said to be $q : p$ phase locked if the rotation number $\rho(f) = \frac{p}{q}$.

Phase locking is also referred to as "mode locking" in [2,3].

When $B = 0$, it is easy to derive the (nonintersecting) level curves of ρ which foliate the (S, σ)-plane (initially derived in [10]). In this case,

$$\tau_{n+1} = \tau_n + 2\pi\rho.$$

Using (5), (7) and $\tau_{n+1} = f(\tau_n)$, the condition above can be written:

$$e^{\sigma(\tau_n + 2\pi\rho)}\left(1 - \frac{\sigma}{S}\right) = e^{\sigma\tau_n}.$$

Solving for S, one finds the following expression relating σ, S, and ρ:

$$S = S_\rho(\sigma) \equiv \frac{\sigma e^{2\pi\sigma\rho}}{e^{2\pi\sigma\rho} - 1}. \tag{9}$$

From (9) it is easy to see that ρ increases (strictly) in a direction transverse to these level curves.

3.1 Analytic Approximations for $n : 1$ phase locking

In this subsection we derive small B approximations for the map f and the regions where $n : 1$ phase locking occurs. Specifically, we will show that the phase locking regions in (σ, S, B) space terminate in a quadratic cusp on $B = 0$ plane for any n. In the subsequent subsection 3.2, we apply our more general theory to the case $n = 2$ and explicitly compute the $2 : 1$ phase lock region. The work presented here should be distinguished from the work by Keener *et. al.* [10] where (for all B) an exact analytic expression for the boundary curves separating regions of $1 : n$ phase locking was derived (rotation number $\rho = n$). Further, we refer the reader to Coombes and Bressloff [2,3] where boundary curves separating $p : q$ phase locking regions in parameter space were computed numerically. There, Arnold tongues eminating from $S = S_\rho$ curves are illustrated.

When $B = 0$, (9) implies that $n : 1$ phase locking (rotation number $\rho = \frac{1}{n}$) can occur only if

$$S = \bar{S}_n(\sigma) \equiv \frac{\sigma e^{\sigma T_n}}{e^{\sigma T_n} - 1}, \quad T_n \equiv \frac{2\pi}{n}. \tag{10}$$

For sufficiently small $B > 0$, the implicit function theorem implies that F is invertible and that the function f in (7) is well defined. We thus seek an approximation of $n : 1$ phase locking regions for $0 < B \ll 1$ near the curves in (10) by assuming expansions of S, B and f of the form:

$$S = \bar{S}_n(\sigma) + \epsilon S_1 + \epsilon^2 S_2 + \cdots \tag{11}$$

$$B = \epsilon B_1 + \epsilon^2 B_2 + \cdots \tag{12}$$

$$f(\tau) = f_0(\tau) + \epsilon f_1(\tau) + \epsilon^2 f_2(\tau) + \cdots \tag{13}$$

where $0 < \epsilon \ll 1$.

Once $f_j(\tau), j = 1, 2$, have been found, the phase lock condition can be expanded in ϵ as follows:

$$\tau + 2\pi = f^n(\tau, \epsilon) = F_{n,0}(\tau) + \epsilon F_{n,1}(\tau) + \epsilon^2 F_{n,2}(\tau) + \cdots \tag{14}$$

Since this equation must be satisfied to all orders in ϵ, the conditions $F_{n,j} = 0, j = 1, 2$ will yield the necessary conditions relating B_j and S_j to expose the "tongue" structure of the $n : 1$ phase locking region. Toward this end, we shall make use of the following Lemmas:

Lemma 3 *Let $f = f(\tau, \epsilon), f : \mathbb{R}^2 \to \mathbb{R}$, be smooth and have the expansion*

$$f(\tau) = (\tau + a) + \epsilon f_1(\tau) + \epsilon^2 f_2(\tau) + O(\epsilon^3)$$

for some constant a and ϵ sufficiently small. Then, for $n \geq 2$,

$$f^n(\tau) = F_{n,0}(\tau) + \epsilon F_{n,1}(t) + \epsilon^2 F_{n,2}(t) + O(\epsilon^3)$$

where

$$F_{n,0}(\tau) = \tau + na$$

$$F_{n,1}(\tau) = \sum_{j=0}^{n-1} f_1(\tau + ja)$$

$$F_{n,2}(\tau) = \sum_{j=0}^{n-1} f_2(\tau + ja) + \sum_{k=1}^{n-1} f_1'(\tau + ka) \sum_{i=0}^{k-1} f_1(\tau + ia)$$

Proof. The proof is inductive. $\square$

8

Lemma 4 *For all $\tau \in \mathbb{R}$ and integers $n \geq 2$*

$$\sum_{k=0}^{n-1} \sin\left(\tau + kT_n\right) = \sum_{k=0}^{n-1} \cos\left(\tau + kT_n\right) = 0, \quad T_n = \frac{2\pi}{n}. \tag{15}$$

Proof. The n roots of $P_n(z) = z^n - 1$ are $z_k = e^{2\pi i k/n}$, $i^2 = -1$, $k = 0, 1, \ldots, n-1$. In the expansion

$$P_n(z) = \prod_{k=0}^{n-1}(z - z_k) = \sum_{k=0}^{n-1} a_k z^k,$$

only the coefficients a_n and a_0 are nonzero. Since $a_{n-1} = -\sum_{k=0}^{n-1} z_k$,

$$-a_{n-1} = \sum_{k=0}^{n-1} z_k = \sum_{k=0}^{n-1} \cos\left(kT_n\right) + i \sum_{k=0}^{n-1} \sin\left(kT_n\right) = 0$$

so that

$$\sum_{k=0}^{n-1} \cos\left(kT_n\right) = \sum_{k=0}^{n-1} \sin\left(kT_n\right) = 0$$

The lemma follows by using this last result and trigonometric addition formulae to expand the sums in (15). $\square$

We start the construction of the expansion (14) by computing f_0 using $B = 0$ in (7), i.e., $f_0(\tau) = f(\tau)$ for $B = 0$. This results in:

$$f_0(\tau) = \tau + a \quad , \quad a \equiv \frac{1}{\sigma} log\left(\frac{S}{S - \sigma}\right), \quad B = 0.$$

An $n : 1$ phase lock can occur only if there exists a $\tau \in (0, 2\pi)$ such that

$$\tau + 2\pi = f_0^n(\tau) = \tau + na \tag{16}$$

where f_0^n denotes the nth composite of f_0 with itself.

The condition defining the map f for the firing times is

$$\Delta(z, S, B) \equiv F(z) - F(\tau) - \frac{\sigma}{S} e^{\sigma\tau} = 0 \quad , \quad z = f(\tau),$$

where F is defined in (5). Using the expansions (11)-(13), we define

$$\delta(\epsilon) = \Delta(f_0 + \epsilon f_1 + \epsilon^2 f_2 + \cdots, \bar{S}_n + \epsilon S_1 + \epsilon^2 S_2 + \cdots, \epsilon B_1 + \epsilon^2 B_2 + \cdots)$$

Because of how $\bar{S}_n$ and a are defined, $\delta(0) = 0$. Moreover, note that

$$a = \frac{2\pi}{n}.$$

9

Next we determine f_1 and f_2 from the conditions $\delta'(0) = 0$ and $\delta''(0) = 0$, respectively.

The first of these conditions is

$$\delta'(0) = \Delta_z^0 f_1 + \Delta_S^0 S_1 + \Delta_B^0 B_1 = 0$$

where $(\ )^0$ denotes the evaluation $(z, S, B) = (\tau + a, \bar{S}_n, 0)$ and the subscripts are derivatives. Solving this for f_1, one finds

$$f_1(\tau) = \alpha_{s,1} S_1 + \alpha_{b,1}(\tau) B_1$$

where

$$\alpha_{s,1} = \frac{1}{\bar{S}_n(\sigma - \bar{S}_n)}, \tag{17}$$

$$\alpha_{b,1}(\tau) = a_{b,1}, \left(\sin(\tau + a + \beta) - e^{-\sigma a} \sin(\tau + \beta) \right)$$

and

$$a_{b,1} \equiv \frac{\bar{S}_n \sin(\beta)}{\sigma(\sigma - \bar{S}_n)}.$$

Given Lemma 3, $F_{n,1}$ in (14) is given by:

$$F_{n,1}(\tau) = \sum_{j=0}^{n-1} f_1(\tau + ja).$$

By Lemma 4,

$$\begin{aligned}
F_{n,1}(\tau) &= S_1 \sum_{j=0}^{n-1} \alpha_{s,1} + B_1 \sum_{j=0}^{n-1} \alpha_{b,1}(\tau + ja) \\
&= n S_1 \alpha_{s,1}.
\end{aligned}$$

Since the $O(\epsilon)$ term of (14) must vanish, we conclude

$$S_1 = 0,$$

In the next subsection we derive analytic approximations to expose the Arnold tongue regions eminating from the curves when $\rho = \frac{1}{n}$. so that

$$f_1(\tau) = \alpha_{b,1}(\tau) B_1. \tag{18}$$

Using $S_1 = 0$ in (11)-(12) we see that $|S - \bar{S}_n(\sigma)| = O(\epsilon^2)$ resulting in the relation:

$$|S - \bar{S}_n(\sigma)| = O(B^2).$$

10

This relation is true for all $n = 1, 2, \ldots$ and demonstrates how all $n : 1$ phase lock regions in the (S, B)-plane (for any fixed $\sigma > 0$) terminate in an Arnold tongue with (at least) a quadratic cusp.

We now proceed to compute f_2. Using $S_1 = 0$,

$$\frac{\delta''(0)}{2} = \Delta_z^0 f_2 + \Delta_S^0 S_2 + \Delta_B^0 B_2 + \frac{1}{2}\Delta_{zz}^0 f_1^2 + \Delta_{zB}^0 f_1 B_1 + \frac{1}{2}\Delta_{BB}^0 B_1^2 = 0. \quad (19)$$

Solving (19) for f_2 one finds:

$$f_2(\tau) = \alpha_{s,2} S_2 + \alpha_{B,2}(\tau) B_2 + \gamma_1 f_1(\tau)^2 + \gamma_2(\tau) B_1 f_1(\tau) \quad (20)$$

where

$$\begin{aligned}
\alpha_{s,2} &= \alpha_{s,1} \\
\alpha_{b,2}(\tau) &= \alpha_{b,1}(\tau) \\
\gamma_1 &= -\frac{1}{2}\sigma \\
\gamma_2(\tau) &= a_{b,1}\left(\sin(\tau + a + \beta) + \cos(\tau + a + \beta)\right)
\end{aligned}$$

In principle, the expressions for f_1 and f_2 can be used in conjunction with Lemma 3 to compute an explicit formula for $F_{n,2}$ for a general n. In the next subsection we illustrate this procedure for the $n = 2$ case. Explicit formulae for the $n > 2$ case remain illusive.

3.2   Application to $2 : 1$ phase locking

In this subsection we derive the firing time map for the 2:1 phase lock. For $n = 2$, $a = \pi$ so that the expressions (18) and (20) become (after simplification)

$$f_1(\tau) = -a_{b,1} \sin T \left(1 + e^{-\sigma\pi}\right) B_1 \quad (21)$$

$$f_2(\tau) = \alpha_{s,1} S_2 - a_{b,1} \sin T \left(1 + e^{-\sigma\pi}\right) B_2 + f_1'(\tau) f_1(\tau) \quad (22)$$

where

$$T \equiv \tau + \beta.$$

Using these specific forms to define the expansion of the firing time map f, the associated expansion for f^2 can then be determined. Because $S_1 = 0$, $F_{2,1} = 0$. The higher order term $F_{2,2}$ can then be obtained by using (21)-(22) and Lemma 3. On account of Lemma 4, however, it is clear that the coefficient of $F_{2,2}$ in B_2 is zero. Also, because f_1 is linear in B_1 then Lemma 3 and (22) imply that $F_{2,2}$ is

11

quadratic in B_1. Specifically, $F_{2,2}$ has the form

$$F_{2,2} = 2\alpha_{s,1}S_2 + a_{b,1}^2 c_{b,1}(T)B_1^2 \tag{23}$$

Moreover, because f_1 is linear in $\sin T$, $F_{2,2}$ is at most quadratic in $\sin T$ and $\cos T$. Thus, $c_{b,1}(T)$ has a Fourier expansion

$$c_{b,1}(T) = a_0 + \sum_{k=1}^{2}(a_k \cos kT + b_k \sin kT) \tag{24}$$

Explicit calculations then reveal:

$$a_0 = \left(1 - \frac{1}{2}\sigma\right) + (1 - \sigma)e^{-\sigma\pi} - \frac{1}{2}\sigma e^{-2\sigma\pi} \tag{25}$$

$$a_1 = 0 \tag{26}$$

$$a_2 = -a_0 \tag{27}$$

$$b_1 = 0 \tag{28}$$

$$b_2 = \frac{1}{2}\left(1 - e^{-2\sigma\pi}\right) \tag{29}$$

For the $2:1$ phase lock condition (14) to be satisfied to all orders in ϵ, $F_{2,2}$ must vanish. Thus, for ϵ sufficiently small, there will be a $2:1$ phase lock only if

$$F_{2,2} = F_{2,2}(\tau; \sigma, B_1, S_2) = 0$$

has a root $\tau \in [0, 2\pi)$. The existence of such a root depends on the parameters (σ, B_1, S_2). From (23)-(29) we see that there exist τ independent functions $\bar{A}, \bar{B}$ and $\bar{C}$ such that

$$F_{2,2} = \bar{A} + \bar{B}\cos(2T) + \bar{C}\sin(2T)$$
$$= \bar{A} + \sqrt{\bar{B}^2 + \bar{C}^2}\left(\frac{\bar{B}}{\sqrt{\bar{B}^2 + \bar{C}^2}}\cos(2T) + \frac{\bar{C}}{\sqrt{\bar{B}^2 + \bar{C}^2}}\sin(2T)\right).$$

Therefore, $F_{2,2}$ can be written in the amplitude-phase form

$$F_{2,2} = \bar{A} + \sqrt{\bar{B}^2 + \bar{C}^2}\cos 2(T - T_0) \quad , \quad T = \tau + \beta, \tag{30}$$

for some T_0. From (30) it is evident that $F_{2,2}$ has a real root τ only if $\cos 2(T - T_0) \in (-1, 1)$, or that

$$\lambda \equiv \frac{\bar{A}}{\sqrt{\bar{B}^2 + \bar{C}^2}} \in (-1, 1).$$

Using (23)-(29), one finds

$$\lambda(\sigma, B_1, S_2) = \frac{2\alpha_{s,1}S_2 - a_2 a_{b,1}^2 B_1^2}{a_{b,1}^2\sqrt{a_2^2 + b_2^2 B_1^2}} \tag{31}$$

12

Using (31), the solvability condition $\lambda(\sigma, B_1, S_2) = \alpha \in (-1, 1)$ is equivalent to

$$S_2 = D(\sigma, \alpha) B_1^2 \tag{32}$$

where

$$D(\sigma, \alpha) = m(\alpha - \alpha^*) \quad , \alpha \in (-1, 1)$$
$$m(\sigma) = \frac{a_{b,1}^2 \sqrt{a_2^2 + b_2^2}}{2\alpha_{s,1}}$$
$$\alpha^*(\sigma) = \frac{-a_2}{\sqrt{a_2^2 + b_2^2}}$$

The region Ω spanned out by (32) for $\alpha \in (-1, 1)$ defines those (σ, B_1, S_2) for which $F_{2,2} = 0$ has a real root τ and thus describes those (σ, B, S) with S near $\bar{S}_n$ for which a 2:1 phase lock occurs (in the limit $B \to 0$).

Using (17) and (10), it is easily verified that $\alpha_{s,1} < 0, \forall \sigma > 0$. Then, since

$$\frac{\partial D}{\partial \alpha} = m < 0,$$

the region Ω is bounded by the two parabolic sheets $S_2 = D(\sigma, 1) B_1^2$ and $S_2 = D(\sigma, -1) B_1^2$. A cross section of this region is shown in Figure 2 for a fixed σ value. This figure illustrates a quadratic cusp shape ("tongue") which is qualitatively similar for all $\sigma > 0$. Specifically, when $B_1 > 0$, 2:1 phase locking occurs for both positive and negative S_2 for all $\sigma > 0$. This fact is readily verified by noting that $\alpha^* \in (-1, 1)$ for $\sigma > 0$.

4 Approximate phase locking for Rössler attractor

The goal of this section is to show, first, that the input $S_R(t)$ garnered from the Rössler attractor can be approximated by a periodic input $S_P(t)$. Further, if we compute the $2 : 1$ Arnold tongue for the input $S_P(t)$, there is an open set of parameters nearby where the Rössler driven IF exhibits approximate phase locking. This is manifested by the fact that the attractor of the discrete map g is a strict subset of the Rössler attractor. This explains Figure 1B.

We will also make a numerical exploration of the parameter space where the $5 : 1$ Arnold tongue is expected. However, we lack the analytical expression for the tongue and consequently our results are less conclusive.

We start with the observation that the definition of phase locking, as presented in the previous section, does not make sense for the input $S_R(t)$. Indeed, such an input
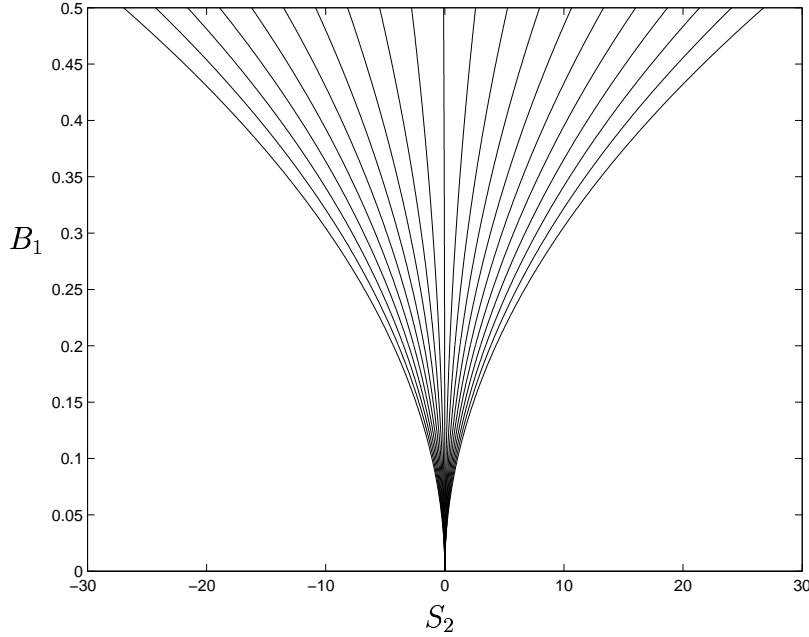
13

Fig. 2. Figure shows the (S_2, B_1) for which 2:1 phaselocking occurs ($\sigma = 2$) in the limit as $\epsilon \to 0$. Specifically, the family of curves graphed are $S_2 = D(1, \alpha_k) B_1^2, \alpha_k = -1 + \frac{k}{10}, k = 0, 1, \ldots 20$. Along each of these curves, the solvability condition (14) is satisfied to $O(\epsilon^2)$ for some τ and $n = 2$.

does not have a period over which the average number of fires can be counted. On the other hand, as we will see in a moment, the input $S_R(t)$ closely resembles a periodic function.

There are two sets of parameters related to our discussion. The set of parameters (a, b, c) affecting the behavior of the Rössler attractor will be fixed. The remaining parameters are the scaling parameters $\hat{S}$ and $\hat{B}$ used in the construction of the signal $S_R(t)$ and the leak constant σ in the integrate-and-fire model. We shall use the notation $\hat{\lambda} = (\hat{\sigma}, \hat{S}, \hat{B})$ to refer to the parameters used when forcing the IF model with $s(t) = S_R(t)$ and with $\sigma = \hat{\sigma}$.

Also, for the rest of this paper we fix the initial condition in the Rössler system as $p_0 := (1, 1, 1)$. Then, the dynamics of g are determined solely by the choice of $\hat{\lambda}$ since the *Rössler parameters* (a, b, c) and p_0 remain unchanged.

To relate the non-periodic signal $S_R(t)$ to a periodic one we do the following construction. The Rössler component $x(t)$ is stored numerically as a time series with N evenly spaced time steps of length Δt. Letting $\mathcal{F}[x(t)]$ denote the discrete Fourier transform of $x(t)$, the transform of S_R is easily computed using the linearity of

14

$\mathcal{F}[\cdot]$:

$$\mathcal{F}[S_R(t)] = \hat{S}\left(1 + \hat{B}\mathcal{F}[x(t)]\right).$$

The Fourier approximation yields,

$$\mathcal{F}[x(t)] = a_0 + \sum_{k=1}^{N}(a_k \cos(\omega_k t) + b_k \sin(\omega_k t)) \tag{33}$$

where a_k and b_k are amplitudes and the frequencies $\omega_k = 2\pi k/(N\Delta t)$.

As can be seen in Figure 3, the power spectrum of $\mathcal{F}[x(t)]$ has a single dominant peak. Let the j-th mode be the dominant mode and define

$$x_j(t) = a_0 + a_j \cos(\omega_j t) + b_j \sin(\omega_j t).$$

Combining terms we get,

$$x_j(t) = a_0 + \sqrt{a_j^2 + b_j^2}\cos(\omega_j(t - t_0))$$

where $t_0 = \frac{1}{\omega_j}\arctan\left(\frac{b_j}{a_j}\right)$. Since we are interested only in long term behavior which is not affected by the phase shift t_0, we set $t_0 := 0$.
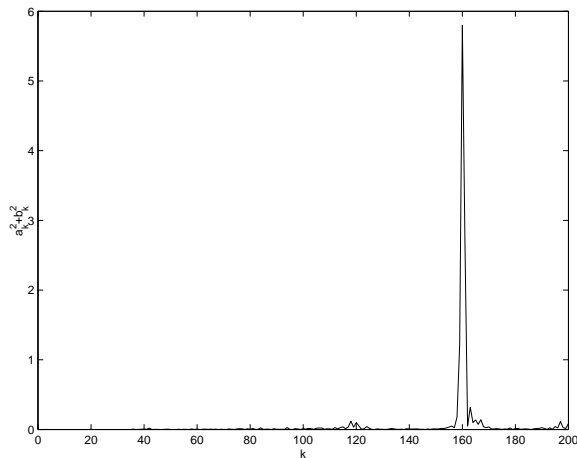

Fig. 3. Power Spectrum for Fourier Transform of Rössler Attractor

This completes a transformation from the signal $x(t)$ to the $\frac{2\pi}{\omega_j}$ periodic, dominant mode approximation $x_j(t)$. We intend to compare solutions to the IF model with the input $S_R(t) = \hat{S}(1 + \hat{B}x(t))$ in

$$\frac{du}{dt} = -\hat{\sigma}u + S_R(t) = -\hat{\sigma}u + \hat{S}(1 + \hat{B}x(t))$$

to solutions of the same equation, where $x(t)$ is replaced by $x_j(t)$ in

$$\frac{du}{dt} = -\hat{\sigma}u + \hat{S}(1 + \hat{B}x_j(t)). \tag{34}$$

15

We note, however, that results of section 3 are applicable only to periodic forcing functions with period 2π and $x_j(t)$ is not 2π periodic. After rescaling, however, time solutions of (34) are identical to solutions of

$$\frac{du}{d\tau} = -\sigma u + S_p(\tau) := -\frac{\hat{\sigma}}{\omega_j} u + \frac{\hat{S}}{\omega_j}\left(1 + \hat{B}x_j\left(\frac{\tau}{\omega_j}\right)\right) \tag{35}$$

where $x_j\left(\frac{\tau}{\omega_j}\right) = a_0 + \sqrt{a_j^2 + b_j^2}\cos(\tau)$. Therefore, we can compare solutions of

$$\frac{du}{dt} = -\hat{\sigma}u + \hat{S}(1 + \hat{B}x(t))$$

to solutions of

$$\frac{du}{d\tau} = -\sigma u + S(1 + B\cos(\tau))$$

where

$$\sigma = \frac{\hat{\sigma}}{\omega_j}$$

$$S = \frac{\hat{S}}{\omega_j}(1 + \hat{B}a_0)$$

$$B = \frac{\hat{B}\sqrt{a_j^2 + b_j^2}}{1 + \hat{B}a_0} \tag{36}$$

Numerically, it was found that for a data set with length $N = 10001$ and $\Delta t = .10$, then $j = 160$, $a_0 \simeq 0.195$, $a_j \simeq -.149$, $b_j \simeq -2.403$ and $\omega_j \simeq 1.006$.

4.1 2 : 1 *locking*

Suzuki *et. al.* showed that for $(\hat{\sigma}, \hat{S}, \hat{B}) = (2, 2, 1/40)$, firing on the Rössler attractor was limited to two distinct 'lines' (see Figure 1). In this subsection we demonstrate numerically that this is not an isolated phenomena, instead occurring on a set of non-empty interior. We will also present evidence that this behavior is a perturbation of $2 : 1$ phase locking in the periodic approximation $S_P(\tau)$.

Using the results of section 3, we will begin by analytically computing the $2 : 1$ phase locking region in (σ, S, B) space and then transforming it into $(\hat{\sigma}, \hat{S}, \hat{B})$ parameter space using (36). For purposes of comparison to Suzuki *et. al.*, we use $\hat{\sigma} = 2$. Therefore, we will choose $\sigma = 2/\omega_j$ in (32). The resulting tongue in $(\hat{\sigma}, \hat{S}, \hat{B})$ parameter space is plotted as a solid line in Figure 4. Also plotted is a numerically calculated region in which the Rössler attractor is "approximately" 2:1 phase locked. The term phase locking implies the existence of a rotation number, a quantity which is not defined for non-periodic input. To generalize this definition, we

16

first fix a Poincarè section Σ of the Rössler attractor defined by $x = 0, \dot{x} < 0$. The trajectory $p(t) = (x(t), y(t), z(t))$ used to generate the input $S_R(t) = \hat{S}(1 + \hat{B}x(t))$, visits the crossection Σ infinitely many times. Let $T_1 < T_2 <, \ldots$ be times such that $p(T_j) \in \Sigma$ for all j. We compute $1/\rho^*$ as the average number of fires between successive visits of trajectory $p(t)$ to Σ for large N, that is

$$\frac{1}{\rho^*} := \lim_{N \to \infty} \frac{\max\{k : \tau_k \le T_N\}}{N},$$

if the limit exists. Then ρ^* is an average phase rotation per fire, where phase is determined relative to an average return time to Poincaré section Σ.

With this new tool, the 2:1 Rössler locked tongue in Figure 4 was computed by both visual inspection, to ensure that firing is confined to two bands, and through a computation of ρ^*. Both methods are necessary since visual inspection alone can not rule out more complicated dynamics (i.e. $1 : 1$ locking mixed in with $2 : 1$), while computing ρ^* exactly requires an infinite number of firing times (we chose to use 400). Observe that the region has nonempty interior.

Figure 5 shows a crossection of the approximate phase lock region for fixed values of $(\hat{\sigma}, \hat{S}) = (2, 2.005)$ as a function of $\hat{B}$. Examination reveals a very short initial interval in which the firing is not $2 : 1$ locked followed by a longer interval corresponding to $\hat{B}$ values within the computed tongue in Figure 4. We note that in further numerical experiments (not shown) the value ρ^* is a good predictor of system behavior. For instance, when $\hat{B}$ is choosen so that $\rho^* = 1/8$, the figure analogous to Figure 1 has eight distinct leaves.

Next we will fix $\hat{B}$ and compare ρ^* as a function of $\hat{\sigma}$ along the line $\hat{S} = \hat{\sigma}$. This result is shown in Figure 6. Also shown is the rotation number ρ, for the periodic input $S_P(\tau)$ at the corresponding values of S and σ defined by (36). Observe, that both the Rössler and periodically driven IF model exhibit similar behavior over a large range of $\hat{\sigma}$. The intervals of constancy of ρ^* represent sections of a set with non-empty interior in the parameter space $(\hat{\sigma}, \hat{S}, \hat{B})$ for which the set $L_g(p_0)$ is a strict subset of the Rössler attractor.

4.2 $5 : 1$ phase locking

Ideally, we would like to extend the argument outlined in the previous subsection for $2 : 1$ to the 5-leaf behavior observed in Suzuki *et. al.* and shown in Figure 1. However, we have no comparable analytical method by which to compute the $5 : 1$ Arnold tongue as we did for the $2 : 1$ case. We will thus limit ourselves to several numerical experiments.

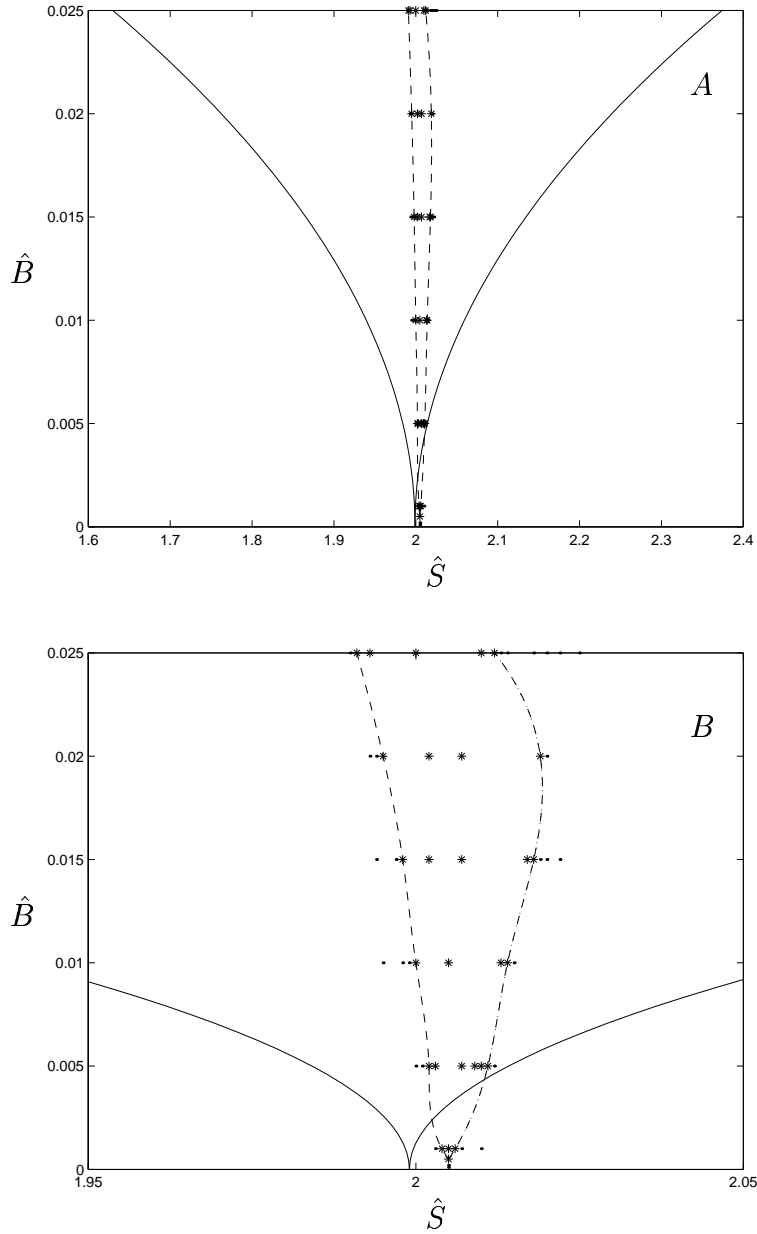Predictably, we begin by looking for $5 : 1$ phase locking in the $S_P(t)$ approximation

Fig. 4. A) A picture of the analytically computed 2 : 1 phase locking tongue transformed into $(\hat{\sigma}, \hat{S}, \hat{B})$ space. Also plotted is the numerically computed 2 : 1 Rössler locked region. The asterisks (*) mark places where the Rössler forced system had two leaves. Dots (·) mark places where the Rössler forced system did not have two leaves. An approximate boundary of this region is plotted as the dotted line. B) Same as A, except a closer view.

of the Rössler attractor at the parameter values which produced the 5-leaf behavior. No such phase locking exists, a fact which is distinctly different from the results of the previous subsection where, at the parameter values suggested by Suzuki *et. al.*, there was a direct correspondence between the limited firing of the Rössler attractor and phase locking of the periodically driven IF model. To explain this difference we return to section 3. There it was noted that all phase locking tongues terminate
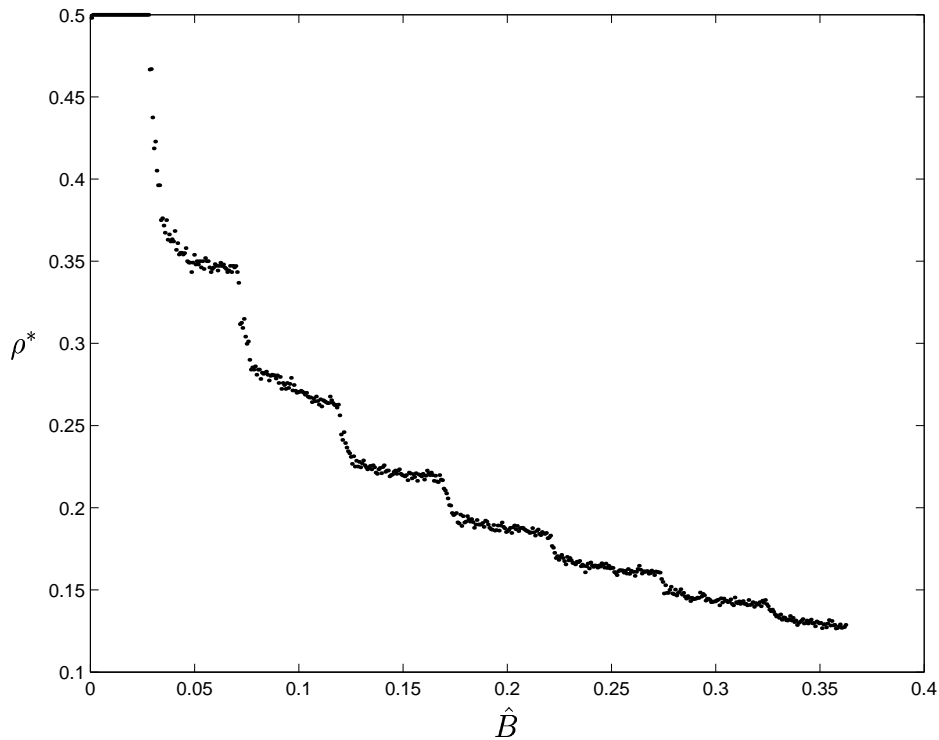
Fig. 5. Plot of average phase rotation ρ^* versus $\hat{B}$ for $(\hat{\sigma}, \hat{S}) = (2, 2.005)$
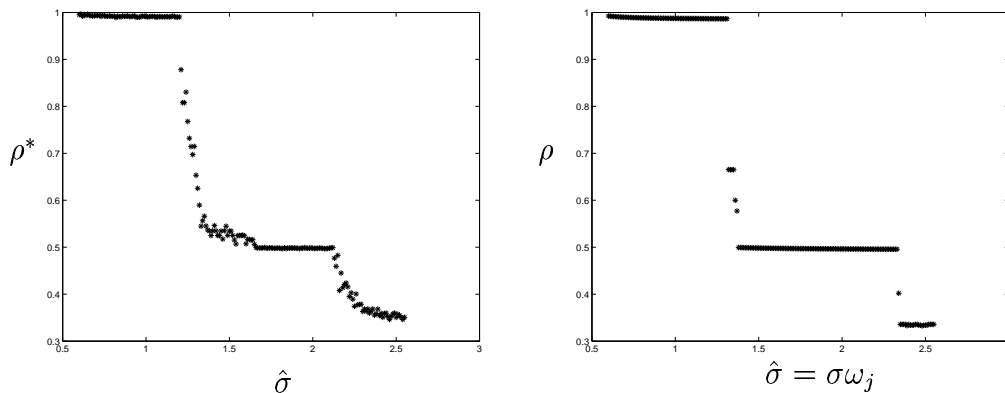

Fig. 6. On the left is the graph of ρ^* vs. $\hat{\sigma}$ for the Rössler forced system for $\hat{S} = \hat{\sigma}$ and $\hat{B} = 1/40$. On the right is the graph of ρ vs. $\hat{\sigma} = \sigma\omega_j$ for the IF model forced by the associated dominant mode of the Fourier Transform.

with a quadratic cusp at $B = 0$. While we can not compute a $5 : 1$ phase locking tongue in this case, we can deduce where the cusp of that tongue is for the $B = 0$ case via (9). The resulting curve is plotted in Figure 7. Selecting points on this curve for $\hat{B} = 1/40$, the periodically forced IF model was $5 : 1$ phase locked, but the Rössler forced IF did not exhibit limited firing confined to five re-
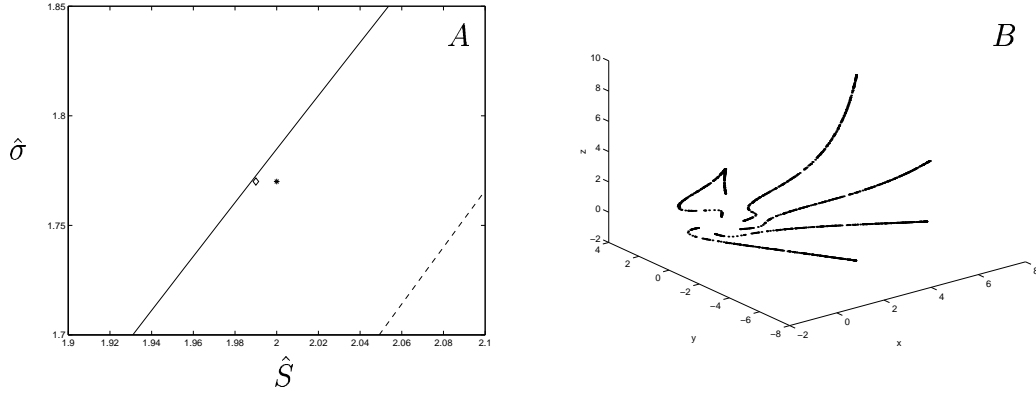
19

Fig. 7. A) Shows curves, after transformation into $(\hat{S}, \hat{\sigma})$-plane, where the IF model forced by the constant input $s(t) = S$ $(B = 0)$ exhibits $5 : 1$ (solid) and $6 : 1$ (dashed) phase locking. Plotted is the parameter pair (asterisk) $(\hat{S}, \hat{\sigma}) = (2.00, 1.77)$, which is the $\hat{B} = 0$ projection of where the five-leaf behavior exists as seen in Figure 1. Note that the corresponding $S_P(t)$ approximation at this point was not $5 : 1$ phase locked. Also plotted (diamond) is the $(\hat{S}, \hat{\sigma}) = (1.77, 1.99)$ pair for which both behaviors are observed. (Figure 7B). B) Firing locations for $(\hat{\sigma}, \hat{S}, \hat{B}) = (1.77, 1.99, .1)$. The five leaf pattern illustrated had a computed value $\rho^* = .2$. For the same parameter values the IF model forced by the associated dominant mode approximation was $5 : 1$ phase locked.

gions. Thus, for this small value of B we observe no known intersection of the two behaviors. However, we note that such correspondence was not always true in the $2 : 1$ case described earlier. Figure 4 showed that for small values of $\hat{B}$ the phase locking regions were not nested. As a consequence, a larger value of $\hat{B}$ may produce the desired correspondence. Indeed, choosing $(\hat{\sigma}, \hat{S}, \hat{B}) = (1.77, 1.99, .1)$ we found that the Rössler attractor exhibited limited firing in the form of five distinct bands. Also, the corresponding dominant mode approximation $S_P(t)$ defined by $(\sigma, S, B) = (1.759, 2.017, .236)$ was $5 : 1$ phase locked. Other points in parameter space were also found to exhibit both behaviors.

In conclusion, while we are unable to derive the $5 : 1$ phase locking tongue for comparison, we are able to show that these behaviors exist nearby and in many cases simultaneously.

The numerics in this subsection confirm that there is a set of parameters with nonempty interior where Rössler driven IF exhibits approximate phase locking.

5 Attractor reconstruction using interspike intervals

In this section we develop a theoretical framework which shows that interspike interval reconstruction can only reconstruct attractor of a discrete map g. We also compare attractor reconstruction using interspike intervals with the reconstruction using delay coordinates.

We proceed now to define the reconstruction map r^i using interspike interals and then the reconstruction map r^d using delay coordinates. For convenience we will use the Rössler attractor in the construction, but it can be applied to a general attractor under a flow or a homeomorphism.

Recall that X is a compact neighborhood of an attractor $\mathcal{A}$ and let $\varphi(t, \cdot)$ be a flow on X. Let $p_0 \in X$ and let $\varphi(t, p_0)$ be a solution of (3) with initial condition $p(\tau_0) = p_0$. Let $\{\tau_i\}_{i=1}^{\infty}$ be the associated sequence of firing times. We assume that the parameters in (1) and (3) are selected in such a way that this sequence is infinite. Let $\beta^i : X \to \mathbf{R}^{\infty}$ be a map associating to a point p_0 a sequence of interspike distances

$$\beta^i(p_0) = \tau := (\tau_1 - \tau_0, \tau_2 - \tau_1, \ldots)$$

and let σ be shift map on a sequence τ

$$\sigma\big((\tau_1 - \tau_0, \tau_2 - \tau_1, \ldots)\big) = (\tau_2 - \tau_1, \tau_3 - \tau_2, \ldots).$$

Let $P_k : \mathbf{R}^{\infty} \to \mathbf{R}^k$ be a projection onto first k components. We will call the map

$$r^i := P_k \circ \beta^i$$

the *interspike interval reconstruction map*. The map r^i maps a neighborhood X of the attractor $\mathcal{A}$ to the reconstruction space $\mathbf{R}^k$.

A similar formulation can be used for delay coordinate reconstruction, originally due to Packard *et. al.* [11]. Once again, let $p_0 \in X$ and let $\varphi(t, p_0)$ be a solution of (3) with initial condition $\varphi(\tau_0, p_0) = p_0$. Select a constant $\alpha > 0$ and a map $y : X \to \mathbf{R}$. Let $\beta^d : X \to \mathbf{R}^{\infty}$ be a map associating to a point p_0 a projection (via the map y) of a sampling of a trajectory $\varphi(t, p_0)$ at multiples of α

$$\beta^d(p_0) = (y(\varphi(\tau_0, p)), y(\varphi(\tau_0+\alpha, p)), y(\varphi(\tau_0+2\alpha, p)), \ldots, y(\varphi(\tau_0+k\alpha, p)), \ldots).$$

Let $P_k : \mathbf{R}^{\infty} \to \mathbf{R}^k$ be, as before, a projection onto first k components. We will call the map
$$r^d := P_k \circ \beta^d$$
the *delay reconstruction map*. Notice that the difference between the maps r^d and r^i is in the way how the time series associated to p_0 is created. In one case, it is the interspike intervals of the IF model driven by input $\varphi(t, p_0)$. In the other case, it is

a sampling of a trajectory in multiples of α, followed by a projection. Both maps r^i and r^d are continuous by continuous dependence on initial conditions.

Definition 5 The set

$$\omega(p) := \{q \in X \mid \text{ there is a sequence } t_i \to \infty \text{ with } \varphi(t_i, p) \to q\}$$

is called the ω-limit set of p under flow.

Definition 6 ([13]) A set E is called *residual* if its complement is a countable union of nowhere dense sets. A property is called *generic* if it holds for a residual subset of a set of parameters under consideration.

For the rest of this section we assume that the initial condition p_0 is such that $\omega(p_0) = \mathcal{A}$. This is not a restrictive assumption as it is believed to hold for all strange attractors for generic choice of p_0 in the basin of attraction.

In applications a time series (sequence $\beta(p_0)$) is given and the goal is to reconstruct the unknown attractor $\mathcal{A}$ or some of its features such as dimension, characteristic exponents and entropy [4,7,8,19]. A selection of k is made arbitrarily and then the projection of the sequence $\beta(p_0)$ and its shifts $\sigma^n(\beta(p_0))$ to $\mathbf{R}^k$ serves as a reconstruction of $\mathcal{A}$. It is clear that if the map r^d is not injective information is lost during the reconstruction. Therefore, a great deal of effort has been expended to show injectivity of r^d. A classical results of Takens [18](Corollary 5) (see also [16]) shows that generically (in a certain space of parameters) r^d is injective for suficiently large k.

Sauer [15] proved a similar result for map r^i in the case when the interspike interval sequence is produced by the IF model without leak ($\sigma = 0$). In this case, it is once again generically expected that the reconstruction map r^i is injective for a sufficiently large embedding dimension.

We expect that the map r^i produced by the IF model with leak is injective but that is not focus of this paper. We will not seek to extend these results to IF models with $\sigma \neq 0$. The main point we want to make is that even if the reconstruction map r^i is injective, the reconstruction may fail. In other words, injectivity of r^i is a necessary, but not a sufficient condition for a faithful reconstruction. Therefore for the rest of this section we assume that both r^d and r^i are injective. The following Lemma and some results later in the section hold for both maps r^i and r^d. We shall use notation r with no superscript when the results are valid for both maps.

Lemma 7 *Assume that the reconstruction map r is injective on X. Let $U := r(X)$,*

$U \subset \mathbf{R}^k$. *Then the diagram*

$$
\begin{array}{ccc}
X & \xrightarrow{g} & X \\[4pt]
\beta \downarrow & & \beta \downarrow \\[4pt]
\mathbf{R}^\infty & \xrightarrow{\sigma} & \mathbf{R}^\infty \\[4pt]
P_k \downarrow & & P_k \downarrow \\[4pt]
U & \xrightarrow{G} & U
\end{array}
\tag{37}
$$

commutes, where the map G is defined by

$$
G(x) = P_k(\sigma(P_k^{-1}(x))). \tag{38}
$$

Proof. Take an arbitrary point $p \in X$. We discuss first the case of interspike interval reconstruction. In this case $g = g^i$, $\beta = \beta^i$, $r = r^i$ and $G = G^i$. The point $g^i(p)$ is the point on the attractor at the time of the nearest firing, i.e. at the time τ_1. Therefore the sequence $\beta^i(g^i(p))$ is $(\tau_2 - \tau_1, \tau_3 - \tau_2, \ldots)$ by definition of β^i. It follows that the first square commutes. Since r^i is injective the map P_k is injective on the set $\beta(X)$ as well. It follows that the map G^i is well defined on the set $U = r^i(X)$.

Now we discuss the case of delay reconstruction i.e $g = g^d$, $\beta = \beta^d$, $r = r^d$ and $G = G^d$. The point $g^d(p)$ is the point on the attractor at the time $\tau_0 + \alpha$, starting from initial condition p at time τ_0. Therefore the sequence $\beta^d(g^d(p))$ is $(y(\varphi(\tau_0 + \alpha, p)), y(\varphi(\tau_0 + 2\alpha, p)), \ldots)$ by definition of β^d. It follows that the first square commutes. Since r^d is injective the map P_k is injective on the set $\beta^d(X)$ as well. It follows that the map G^d is well defined on the set $U = r^d(X)$.

Finally, the bottom square commutes by definition of the map G. $\qquad \square$

We want to use diagram (37) to precisely characterize the connection between dynamics on $\mathcal{A}$ and the dynamics of the map G in the reconstruction space. We hasten to point out that injectivity of the map r^d does not guarantee that the dynamics generated by the map G^d mirrors the dynamics of the flow φ. By diagram (37), the projection of all shifts $\sigma^n(\beta(p_0))$ to the reconstruction space $\mathbf{R}^k$ corresponds to mapping the trajectory $\{g^n(p_0)\}_{n=0}^\infty$ via the reconstruction map r. The set

$$
\mathcal{G}(g, p_0) := cl(\{r(g^n(p_0))\}_{n=0}^\infty) \subset U
$$

serves as the reconstruction of $\mathcal{A}$. The map $G : \mathcal{G}(g, p_0) \to \mathcal{G}(g, p_0)$ serves as a reconstruction of the dynamics on $\mathcal{A}$. Notice that if the set U is bounded, i.e. the interspike intervals are uniformly bounded for initial conditions in X, then the set $\mathcal{G}(g, p_0)$ is not empty.

Lemma 8 *Assume that the reconstruction map r is injective on X. Fix $p \in X$ and let $L_g(p)$ be a set of limit points of the sequence $\{g^n(p_0)\}_{n=0}^\infty$. Then the map*

$g : L_g(p) \to L_g(p)$ is conjugate to the map $G : \mathcal{G}(g, p_0) \to \mathcal{G}(g, p_0)$.

Proof.   Observe that by definition of $\mathcal{G}(g, p_0)$ we have

$$\mathcal{G}(g, p_0) = r(L_g(p)).$$

Since r is injective, the function $G : U \to U$ is well defined. Since $L_g(p) \subseteq X$ and $\mathcal{G}(g, p_0) \subseteq U$, the result follows from diagram (37).   □

Corollary 9 *Select $p \in X$, assume $\omega(p) = \mathcal{A}$ and that the reconstruction map r is injective on X. Then, if $L_g(p) = \omega(p)$, the map $G : \mathcal{G}(p_0, g) \to \mathcal{G}(p_0, g)$ is conjugate to the map $g : \mathcal{A} \to \mathcal{A}$.*

The Corollary 9 clearly shows that another key ingredient for faithful reconstruction (apart from injectivity of r) is the requirement that $L_g(p) = \omega(p)$. At this point an essential difference between delay coordinates reconstruction and the reconstruction using interspike distances emerges. For the delay coordinate reconstruction we have a following result.

Theorem 10 ([18], Theorem 4) *Let M be a compact manifold, let X be a vector field on M with flow $\varphi(t, p)$ and let p be a point on M. Then there is a residual set $C_{X,p}$ of positive real numbers, such that if $\alpha \in C_{X,p}$, we have that $\omega(p) = L_\alpha(p)$.*

If p is selected in such a way that $\omega(p) = \mathcal{A}$, this Theorem, together with Corollary 9, shows that delay coordinate reconstruction (generically) works.

However, numerical results from section 4 indicate that there is a set of parameters (Figure 4 and Figure 6) for which the set $L_g(p)$ is a strict subset of $\mathcal{A}$. Since this behavior takes place in regions of the parameter space with non-empty interior, an analog of Theorem 10 does not seem to be true for a map g defined by the interspike intervals of integrate-and-fire model.

We want to conclude this section with a few thoughts on the role of the injectivity of the map r versus the manner in which the time series is produced for the attractor reconstruction problem. We define a *point-by-point reconstruction* of the attractor $\mathcal{A}$. We pick a point $p_0 \in \mathcal{A}$ and compute $r(p_0)$ using the first k elements of $\beta(p_0)$. Then we pick another point p_1 and repeat the process. The reconstructed attractor in $U \subset \mathbf{R}^k$ is

$$\mathcal{D} := r(\mathcal{A}).$$

It is easy to see that if r is injective, the set $\mathcal{D}$ can be justifiably called a reconstruction of $\mathcal{A}$. This should be contrasted to the reconstruction using the induced map G, which we may call *dynamic reconstruction*. For this reconstruction to succeed one needs to show (in addition to injectivity of r) that $L_g(p) = \omega(p)$. Point-by-point reconstruction only reconstructs $\mathcal{A}$ as a set, while dynamic reconstruction also reconstructs the dynamics on $\mathcal{A}$. For comparison of these two approaches see Figure 8. Notice that the parameter values for this figure are the same as in Figure 1A.

Figure 8A also indicates that r^i is injective.

A   B
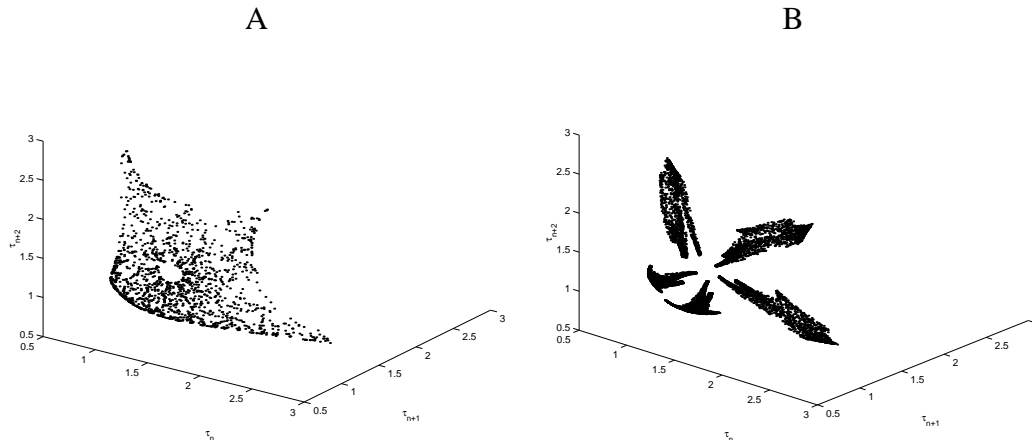

Fig. 8. (A) A point-by-point reconstruction of the Rössler attractor for the parameter set $(\hat{S}, \sigma, \hat{B}) = (2, 1.77, 1/40)$. (B) Dynamic reconstruction of the Rössler attractor at the same value of parameters. The orbit of g can be seen in Figure 1A

In practical applications one is usually given a time series and does not have the data required to attempt a point-by-point reconstruction. That would require multiple data sets with different initial conditions. If the mechanism of time series extraction is not understood and, in particular, if the assumption that the time series is a sampling of a trajectory in regular time intervals is not justified, then our results urge caution. The dynamic reconstruction may only capture part of the attractor in the original system. If there are resources to obtain data for point-by-point reconstruction and the interest is in the set properties of the original attractor, then our results suggest that point-by-point reconstruction may be a more reliable method.

6 Conclusions

This paper had two goals. The first was to observe that dynamic reconstruction of an attractor from the time series data reconstructs only the attractor of a certain discrete map. If this attractor is strict subset of the original attractor, the reconstruction will be incomplete. Suzuki *et. al.* [14] found that the attractor of the discrete map was a strict subset of the Rössler attractor for certain parameter values when the discrete map was generated by integrate-and-fire model and the real neuron as well.

The second goal of this paper was to explain this phenomena as a consequence of the phase locking in the periodically forced integrate-and-fire model, which is in a certain sense close to the aperiodically forced system. Our numerical simulations indicate that there is an open set of parameters for which the discrete attractor is a strict subset of the Rössler attractor. This indicates that, unlike dynamic reconstruction using delay coordinates [18,16], the dynamic reconstruction using interspike

distances is not generic.

The numerical evidence presented in section 4 suggests that the banded structure of $L_g(p)$ can be predicted (for small $\hat{B}$) by $n:1$ phaselocking observed in a "nearby" periodically forced IF model. One reason this worked well for the Rössler forced IF model is that the Fourier spectrum of $x(t)$ was very sharp at a sole dominant mode (see Figure 3). Had the power spectrum been broader, mixing modes of different frequencies would have had similar amplitudes making our single mode approximation less accurate.

One can speculate about the significance of these results as it pertains to neural processing. If we present inputs (to our admittedly simplistic integrate-and-fire model of the neuron) starting at random points on the Rössler attractor, we can reconstruct the attractor from the interspike distances (see Figure 8A). However, if these points are temporary related, as they are if they lie on a single trajectory on the attractor, then the reconstruction of the input will exhibit this temporal structure. In other words, since the signal $S_R(t)$ garnered from the Rössler attractor is close to a periodic signal $S_P(t)$, the neural system will phase lock onto the temporal feature of the output (see Figure 8B).

The results of Suzuki *et. al.* [14] indicate that similar behavior is observed for real neurons and not only IF models. Does this mean that some neurons are specifically selective for the temporal structure of the signal? Is this an evolutionary liability or an advantage? The anwers to these questions go beyond the scope of this paper.

There are outsanding mathematical problems as well. The phenomena of phase locking has been interpreted much more widely in the neuroscience literature than the mathematical definition we have used in this paper. As an example, phase locking has been used [12] to describe post-stimulus spike histograms in response to periodic stimuli, which have similar periodic shape as the driving function. An interesting related mathematical problem is that of making a broader definition of phase locking using a generalized definition of the rotation number ρ^* which is continuous in a large space of functions and for wide class of neuronal models.

References

[1] Brenner N., Bialek W. and de Ruyter van Steveninck R., Adaptive rescaling maximizes information transmission, *Neuron* 26, 695-702, June 2000.

[2] S.-Coombes and P.C. Bressloff, Mode locking and Arnold tongues in integrate-and-fire neural oscillators, *Phys. Rev. E*, vol.60, No.2, (1999), 2086-2096.

[3] S.-Coombes and P.C. Bressloff, Erratum:Mode locking and Arnold tongues in integrate-and-fire neural oscillators, *Phys. Rev. E*, vol.63, No. 5, 059901 (2001).

[4] J.-P. Eckmann and D. Ruelle, Ergodic theory of chaos and strange attractors, *Reviews of Modern Physics*, vol.57, No.3, part I, (1985), 617-656.

[5] Fairhall A., Lewen G., Bialek W. and de Ruyter van Steveninck R., Efficiency and ambiguity in an adaptive neural code, *Nature* 412, 787-792, August 23 2001.

[6] Gerstner W. and Kistler W., *Spiking neuron models: Single neurons, populations, plasticity*, Cambridge University Press (July 2002).

[7] Grassberger, P. and Procaccia, I., Estimating the Kolmogorov entropy from a chaotic signal, *Phys. Rev. A*, **28**, (1983) 2591.

[8] Grassberger, P. and Procaccia, I., Measuring the strangeness of of strange attractors, *Physica D*, **9**, (1983), 189.

[9] Katok, A. and Hasselblat, B., *Introduction to the modern theory of dynamical systems*, Cambridge University Press (1995).

[10] J.P Keener, F.C. Hoppensteadt, J. Rinzel, Integrate and Fire Models of Nerve Membrane Response to Oscillatory Input, *SIAM Journal of Applied Mathematics*, Vol. 41, Issue 3 (1981), 503-517.

[11] Packard, N., Crutchfield J.P., Farmer J.D., Shaw R.S., Geometry from a Time Series, *Physical Review Letters*, Vol. 45, September 1980, 712-716.

[12] Rieke F., Warland D., de Ruyter van Steveninck R. and Bialek W., *Spikes: exploring the neural code*, MIT Press 1997.

[13] Royden, H.L., Real Analysis, 2nd edition. MacMillan Publishing Co., Inc, New York (1968).

[14] H. Suzuki, K. Aihara, J. Murakami, T. Shimozawa, Analysis of neural spike trains with interspike interval reconstruction, *Biological Cybernetics*, Vol. 82,(2000) 305-311.

[15] T. Sauer, Reconstruction of Integrate-and-Fire Dynamics, in: *Nonlinear Dynamics and Time Series*, eds. C. Cutler, D. Kaplan, Fields Institute Publications, AMS (1996).

[16] T. Sauer, J. Yorke and M. Casdagli, Embedology, *J. Statistical Physics*, vol. 65, Nos.3/4, (1991), 579-616.

[17] Simoncelli, E. and Olshausen, B., Natural image statsistics and neural representation, em Annu. Rev. Neurosci. 24, (2001), 1193-1216.

[18] Takens, F., Detecting strange attractors in turbulence, *Dynamical Systems and Turbulence, Warwick 1980* Lecture Notes in Mathematics 898, 366-381.

[19] Young, L-S., Dimension, entropy and Liapunov exponents, *Ergod. Theory Dynam. Syst*, **2**, (1982), 109.